Dalton Transactions

ROYAL SOCIETY OF CHEMISTRY

COMMUNICATION

View Article Online
View Journal | View Issue

Cite this: *Dalton Trans.*, 2024, **53**, 19093

Received 11th October 2024,
Accepted 7th November 2024

DOI: 10.1039/d4dt02848a

rsc.li/dalton

Titanosiloxanes consisting of tetrahedrally coordinated Ti cores and branched siloxane cages†

Shohei Saito,‡[a] Kenta Kawamura,‡[a] Naoto Sato,[a] Takamichi Matsuno,[a,b] Hiroaki Wada,[a] Kazuyuki Kuroda[a,b] and Atsushi Shimojima[*a,b]

Well-defined titanosiloxane molecules with tetrahedrally coordinated Ti centers were synthesized by using monosilanol-functionalized siloxane cages as building blocks. The Ti sites are modified with $-OSi(OSi)_3$ units, which is analogous to Ti-containing zeolites. Such titanosiloxane molecules are important as models for Ti-containing silica-based catalysts.

The bottom-up synthesis of siloxane-based nanomaterials using well-defined building blocks facilitates fine control over their physical properties and the emergence of new functions by molecular design.[1–5] Polyhedral oligomeric silsesquioxanes (POSSs) with a general formula of $(RSiO_{3/2})_n$, where $n \geq 6$ and R = H or organic groups, are widely used as molecular building blocks owing to their rigid frameworks and facile functionalizability.[6–9] Covalent linking of POSSs can afford various siloxane-based materials, such as discrete oligomers[10–17] and porous networks.[18,19] Regioselective functionalization of cage corners is a promising approach for controlling the linked geometries of POSSs.[5–7] Mono-functionalized cubic POSSs ($R'R_7Si_8O_{12}$, R′ = functional groups) are most commonly used as building blocks because they are easily synthesized *via* silylation of incompletely condensed trisilanol POSSs ($R_7(HO)_3Si_7O_9$).[6,7,20] Mono-functionalized cubic POSSs have recently been connected *via* organic linkers to produce giant molecules with well-defined radial[10,11] and dendritic structures.[14,15]

The formation of metallasiloxanes with Si–O–M (M = metal atoms) bonds using POSSs is of significant interest owing to their potential applications as molecular catalysts for a variety of organic reactions.[21] The molecularly defined structures of POSS-based metallasiloxanes also provide important models for heterogeneous catalysts, such as metal-containing zeolites. Metal–POSS complexes, in which one silicon atom at the vertex of the cubic POSS is substituted with a metal atom (*e.g.*, Zr,[22–24] Sn,[23] V,[25] or Ti[24,26–28]), have been well studied because they are easily synthesized by reacting the corresponding trisilanol POSS with a metal source. Previous reports have revealed that the properties of POSS-based metallasiloxanes depend on their coordination numbers as well as steric and electronic effects associated with the ligand.[21,29,30] We recently reported the synthesis of a nanoporous titanosiloxane by three-dimensional (3D) cross-linking of an octasilanol-functionalized cage siloxane ($Si_8O_{12}(OSiMe_2OH)_8$) with titanium tetraethoxide.[31] The Ti sites surrounded by siloxane cages were found to be catalytically active toward cyclohexene oxidation; however, their detailed structures have not been elucidated, which is mainly ascribable to the structural ambiguity associated with the amorphous 3D network.

Herein, we report the synthesis and isolation of well-defined titanosiloxane molecules comprising Ti cores and branched siloxane cages by reacting monosilanol POSSs ($^iBu_7(HO)Si_8O_{12}$) with a titanium source (titanium(IV) chloride ($TiCl_4$) or cyclopentadienyltitanium(IV) trichloride ($CpTiCl_3$)) (Scheme 1). Although a dumbbell-shaped Ti–POSS compound, in which two siloxane cages are bridged by Ti species, has been reported in the literature,[32] the synthesis of branched titanosiloxane molecules comprising three or four cage units is unprecedented. The precise syntheses of such large metallasiloxane compounds containing multiple POSSs pave the way for the modular synthesis of zeolite catalysts containing cage siloxanes as secondary building units.

$^iBu_7(HO)Si_8O_{12}$ was synthesized from a mono-hydride POSS ($^iBu_7HSi_8O_{12}$), which was obtained by reacting an incompletely condensed POSS ($^iBu_7(HO)_3Si_7O_9$) with trichlorosilane ($HSiCl_3$) according to a previously reported procedure.[33] A titanosiloxane molecule consisting of a Ti core and four branched siloxane cages ($(^iBu_7Si_8O_{13})_4Ti$ was synthesized by reacting $^iBu_7(HO)Si_8O_{12}$ with $TiCl_4$ in the presence of Et_3N (Scheme 1). The

[a]*Department of Applied Chemistry, Faculty of Science and Engineering, Waseda University, 3-4-1 Okubo, Shinjuku-ku, Tokyo 169-8555, Japan. E-mail: shimojima@waseda.jp*
[b]*Kagami Memorial Research Institute for Materials Science and Technology, Waseda University, 2-8-26 Nishiwaseda, Shinjuku-ku, Tokyo, 169-0051, Japan*

†Electronic supplementary information (ESI) available: Experimental details, spectral data (^{29}Si NMR, MALDI-TOF MS, and UV–Vis), and crystal data. CCDC 2388983. For ESI and crystallographic data in CIF or other electronic format see DOI: https://doi.org/10.1039/d4dt02848a

‡These authors equally contributed to this work.

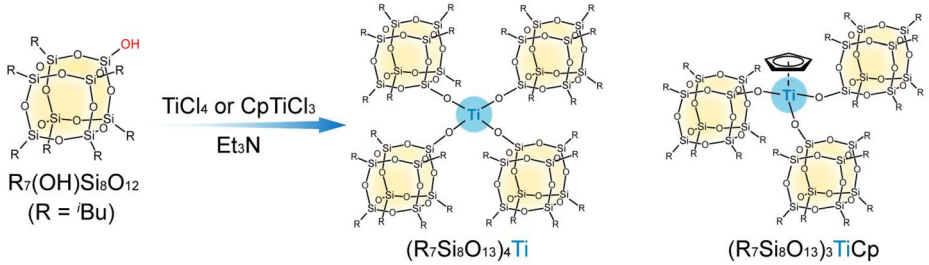

Scheme 1 Synthesis of titanosiloxanes comprising Ti cores and branched siloxane cages.

molar ratio was $^{i}Bu_7(HO)Si_8O_{12}/TiCl_4/Et_3N = 4:1:4.8$. After the reaction at 0 °C for 6 h, the precipitates of $Et_3N{\cdot}HCl$ were removed by filtration and the filtrate was evaporated under reduced pressure. Needle-shaped crystals of $(^{i}Bu_7Si_8O_{13})_4Ti$ were obtained by recrystallization using a binary acetonitrile–toluene solvent (see the ESI† for details).

The ^{29}Si NMR spectrum of a $CDCl_3$ solution of the crystals (Fig. 1a and Fig. S1, ESI†) exhibits T^3 signals ($(SiO)_3Si^{i}Bu$; −66.97, −67.89, and −68.01 ppm) and a higher-field signal attributable to the $(SiO)_3Si(OTi)$ site (−115.15 ppm)[32] with a 3 : 1 : 3 : 1 intensity ratio, consistent with the four inequivalent Si atoms in $(^{i}Bu_7Si_8O_{13})_4Ti$. The matrix-assisted laser desorption/ionization time-of-flight (MALDI-TOF) mass spectrum (Fig. 1b) shows a signal corresponding to the Na^+ adduct of $(^{i}Bu_7Si_8O_{13})_4Ti$ (m/z = 3401.9) (calcd for $C_{112}H_{252}O_{52}Si_{32}TiNa^+$ $[M + Na]^+$: 3400.8). These results indicate that $(^{i}Bu_7Si_8O_{13})_4Ti$ had been successfully synthesized and isolated.

$(^{i}Bu_7Si_8O_{13})_4Ti$ was subjected to single-crystal X-ray diffractometry (Fig. 2a), which revealed that its crystal is monoclinic and in the $P2_1/c$ space group (crystal data are presented in Table S1, ESI†).[34] In addition, four cage-siloxane units were attached to a Ti atom with a tetrahedral geometry (Ti–O lengths and O–Ti–O and Ti–O–Si angles are listed in Tables S2–S4, ESI†). It should be noted that one of the six O–Ti–O angles is 107.3(3)°, which is slightly different from the others (109–111°) (Fig. 2b and Table S3, ESI†). Moreover, one of the four Ti–O–Si angles is 162.7(4)°, which is also slightly different from the others (172–178°) (Fig. 2b and Table S4, ESI†). These results indicate that the tetrahedral structure of $(^{i}Bu_7Si_8O_{13})_4Ti$ is slightly distorted in the crystal, in contrast to the ^{29}Si NMR results that suggest that the four $(SiO)_3Si(OTi)$ sites are chemically equivalent in solution. Distortion is likely to occur in the crystal in order to form a more densely packed crystal structure than can be achieved by an undistorted tetrahedral arrangement. From the perspective of the molecular arrangement in the crystal structure, the molecules are densely packed, with cages arranged to form a wavy structure in the *bc*-plane (Fig. 2c, and Fig. S2 and S3, ESI†). Note that the large amount of disorder is mainly associated with the ^{i}Bu groups in the $(^{i}Bu_7Si_8O_{13})_4Ti$ crystal. Because the position of the metal atom in the siloxane framework is an important factor for metal-containing silica catalysts,[35,36] this well-defined molecular arrangement will be a valuable model of silica-based catalysts.

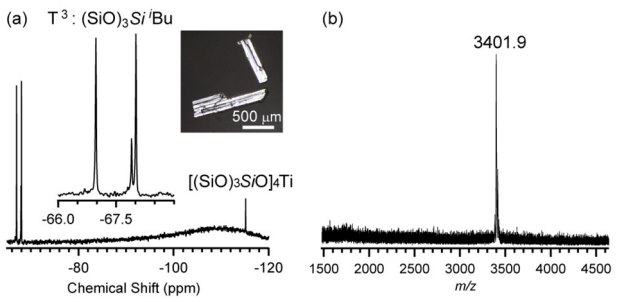

Fig. 1 (a) ^{29}Si NMR and (b) MALDI-TOF MS spectra of $(^{i}Bu_7Si_8O_{13})_4Ti$ after recrystallization. Inset: optical microscopy image of the crystals of $(^{i}Bu_7Si_8O_{13})_4Ti$.

The diffuse reflectance (DR) ultraviolet–visible (UV–Vis) spectrum of $(^{i}Bu_7Si_8O_{13})_4Ti$ (Fig. S4, ESI†) shows a sharp band centered at 210 nm with a broad band at 230–330 nm. The former band is assigned to the ligand-to-metal charge-transfer transition (LMCT) of tetrahedrally coordinated Ti,[28,37,38] while the latter is likely due to the LMCT of octahedrally coordinated Ti,[28,37,38] which is probably formed *via* the partial cleavage of the Si–O–Ti bonds in $(^{i}Bu_7Si_8O_{13})_4Ti$ owing to their instability against moisture[39] and/or pulverization. While we confirmed that pristine $(^{i}Bu_7Si_8O_{13})_4Ti$ crystals are relatively stable in air, a certain degree of deterioration was observed as the crystals were pulverized for DR UV–Vis spectroscopy. The ^{29}Si NMR spectrum of the powdered $(^{i}Bu_7Si_8O_{13})_4Ti$ left to stand in air at room temperature and 40% humidity for 1 d exhibited a signal for $^{i}Bu_7(HO)Si_8O_{12}$, suggesting that some of the Si–O–Ti bonds had cleaved (Fig. S5, ESI†). Although improving stability is an issue that remains to be addressed, $(^{i}Bu_7Si_8O_{13})_4Ti$ is promising as a model of heterogeneous catalysts because tetrahedrally coordinated Ti is known to exhibit effective catalytic activity for a variety of reactions, including olefin epoxidation and polymerization.

We examined varying the number of cage units to further design branched titanosiloxanes. A titanosiloxane molecule consisting of a Ti core and three branched siloxane cages ($(^{i}Bu_7Si_8O_{13})_3TiCp$) was synthesized by reacting $^{i}Bu_7(HO)Si_8O_{12}$ with $CpTiCl_3$ in the presence of Et_3N at the molar ratio of $^{i}Bu_7(HO)Si_8O_{12}/CpTiCl_3/Et_3N = 3:1:3.2$ (see the ESI† for details).

A powder product composed of $(^{i}Bu_7Si_8O_{13})_3TiCp$ and $^{i}Bu_7(HO)Si_8O_{12}$ was obtained after the removal of $Et_3N{\cdot}HCl$

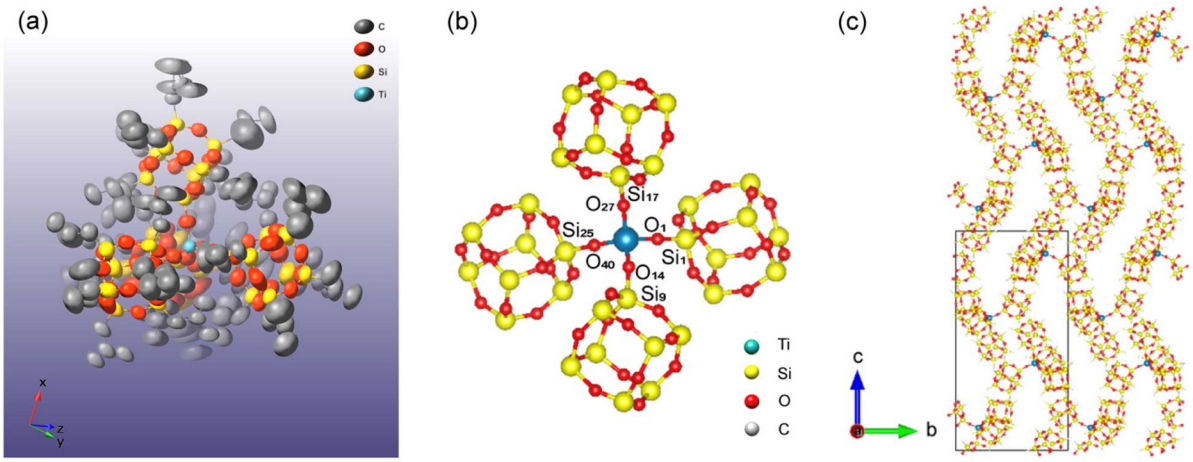

Fig. 2 (a and b) Molecular structure of $(^{i}Bu_7Si_8O_{13})_4Ti$ obtained by single-crystal X-ray diffractometry. Hydrogen atoms are omitted in (a) and both hydrogen and carbon atoms are omitted in (b) for clarity. Color code: yellow, Si; gray, C; red, O. Thermal ellipsoids are drawn at the 30% probability level in (a). (c) Crystal structure of $(^{i}Bu_7Si_8O_{13})_4Ti$ viewed along the *bc* plane. Hydrogen and carbon atoms are omitted for clarity. Color code: blue, Ti; yellow, Si; red, O. CrystalMaker and VESTA (version 3)[40] were used to visualize the structural models.

and the solvent. Unfortunately, unlike $(^{i}Bu_7Si_8O_{13})_4Ti$, crystals of $(^{i}Bu_7Si_8O_{13})_3TiCp$ could not be obtained by recrystallization, and it was isolated using gel permeation chromatography (GPC). The ^{29}Si NMR spectrum (Fig. S6, ESI†) of the product after GPC separation showed a signal at −111.54 ppm, indicative of Si–O–Ti bond formation,[32] and three T^3 signals (−67.06, −67.78, and −67.85 ppm) assignable to the $(SiO)_3Si^{i}Bu$ sites in $(^{i}Bu_7Si_8O_{13})_3TiCp$. The small Q^3 signal is probably due to the hydrolysis of the Si–O–Ti bonds during the GPC separation. MALDI-TOF MS (Fig. S7, ESI†) detected the Na^+ adduct of $(^{i}Bu_7Si_8O_{13})_3TiCp$ (m/z = 2634.5) (calcd for $C_{89}H_{194}O_{39}Si_{24}TiNa^+$ $[M + Na]^+$: 2633.4). These results confirm the formation of $(^{i}Bu_7Si_8O_{13})_3TiCp$. Compared to the four cage units in $(^{i}Bu_7Si_8O_{13})_4Ti$, a molecular structure comprising three siloxane cage units is expected to provide superior accessibility of reactant molecules to the Ti site. Although further molecular design is required to improve the hydrolytic stability of both $(^{i}Bu_7Si_8O_{13})_4Ti$ and $(^{i}Bu_7Si_8O_{13})_3TiCp$, these molecules are potentially important titanosiloxane-based catalysts.

Conclusions

We synthesized $(^{i}Bu_7Si_8O_{13})_4Ti$ and $(^{i}Bu_7Si_8O_{13})_3TiCp$ as a new class of titanosiloxanes consisting of Ti cores and branched siloxane cages by reacting monosilanol POSSs with Ti sources. $(^{i}Bu_7Si_8O_{13})_4Ti$ was determined to have a slightly distorted tetrahedral structure by X-ray crystallography, with cage units arranged in a wave-like structure in the crystal. Because the performance of metal-containing silica catalysts depends on various parameters, including the coordination number of the metal atom, bond length, and bond angles, the precise synthesis of well-defined titanosiloxanes in this study will advance the design of siloxane-based catalysts.

Data availability

Crystallographic data reported in this manuscript have been deposited in the Cambridge Crystallographic Data Centre under supplementary publication no. CCDC 2388983 and can be obtained from **https://www.ccdc.cam.ac.uk/**. The data supporting this article have been included as part of the ESI.†

Conflicts of interest

There are no conflicts to declare.

Acknowledgements

We thank Mr S. Sato, Dr H. Sato (Rigaku Corporation) and Mr T. Goto (Materials Characterization Central Lab., Waseda Univ.) for the X-ray diffraction analysis. We are grateful to the Materials Characterization Central Lab., Waseda Univ. for supporting the NMR and MS measurements. This work was supported in part by Grant-in-Aid for the Strategic International Collaborative Research Program (SICORP) "France-Japan Joint Call on Molecular Technology" from the Japan Science and Technology Agency (JST). This work was also supported in part by JSPS KAKENHI (grant no. 23H02051). S. Saito is thankful to the JX-Waseda Research Fund for Young Researchers.

References

1 C. Sanchez, G. Soler-Illia, F. Ribot, T. Lalot, C. R. Mayer and V. Cabuil, *Chem. Mater.*, 2001, **13**, 3061.
2 X. Yu, K. Yue, I.-F. Hsieh, Y. Li, X.-H. Dong, C. Liu, Y. Xin, H.-F. Wang, A.-C. Shi, G. R. Newkome, R.-M. Ho,

E.-Q. Chen, W.-B. Zhang and S. Z. D. Cheng, *Proc. Natl. Acad. Sci. U. S. A.*, 2013, **110**, 10078.
3 W.-B. Zhang, X. Yu, C.-L. Wang, H.-J. Sun, I.-F. Hsieh, Y. Li, X.-H. Dong, K. Yue, R. Van Horn and S. Z. D. Cheng, *Macromolecules*, 2014, **47**, 1221.
4 Y. Chujo and K. Tanaka, *Bull. Chem. Soc. Jpn.*, 2015, **88**, 633.
5 A. Shimojima and K. Kuroda, *Molecules*, 2020, **25**, 524.
6 D. B. Cordes, P. D. Lickiss and F. Rataboul, *Chem. Rev.*, 2010, **110**, 2081.
7 G. Li, L. Wang, H. Ni and C. U. Pittman Jr., *J. Inorg. Organomet. Polym. Mater.*, 2001, **11**, 123.
8 K. Naka and Y. Irie, *Polym. Int.*, 2017, **66**, 187.
9 Y. Du and H. Liu, *Dalton Trans.*, 2020, **49**, 5396.
10 H. Araki and K. Naka, *Polym. J.*, 2012, **44**, 340.
11 K. Yamamoto, D. Kawaguchi, T. Abe, T. Komino, M. Mamada, T. Kabe, C. Adachi, K. Naka and K. Tanaka, *Langmuir*, 2020, **36**, 9960.
12 S. E. Anderson, C. Mitchell, T. S. Haddad, A. Vij, J. J. Schwab and M. T. Bowers, *Chem. Mater.*, 2006, **18**, 1490.
13 S. Gießmann, A. Fischer and F. T. Edelmann, *Z. Anorg. Allg. Chem.*, 2004, **630**, 1982.
14 X. Wang, Y. Yang, P. Gao, D. Li, F. Yang, H. Shen, H. Guo, F. Xu and D. Wu, *Chem. Commun.*, 2014, **50**, 6126.
15 M. Huang, C.-H. Hsu, J. Wang, S. Mei, X. Dong, Y. Li, M. Li, H. Liu, W. Zhang, T. Aida, W.-B. Zhang, K. Yue and S. Z. D. Cheng, *Science*, 2015, **348**, 424.
16 N. Rey, S. Carenco, C. Carcel, A. Ouali, D. Portehault, M. Wong Chi Man and C. Sanchez, *Eur. J. Inorg. Chem.*, 2019, **27**, 3148.
17 R. Kajiya, S. Sakakibara, H. Ikawa, K. Higashiguchi, K. Matsuda, H. Wada, K. Kuroda and A. Shimojima, *Chem. Mater.*, 2019, **31**, 9372.
18 W. Chaikittisilp, A. Sugawara, A. Shimojima and T. Okubo, *Chem. Mater.*, 2010, **22**, 4841.
19 Y. Kim, K. Koh, M. F. Roll, R. M. Laine and A. J. Matzger, *Macromolecules*, 2010, **43**, 6995.
20 H. Liu, S. Kondo, R. Tanaka, H. Oku and M. Unno, *J. Organomet. Chem.*, 2008, **693**, 1301.
21 R. Murugavel, A. Voigt, M. G. Walawalkar and H. W. Roesky, *Chem. Rev.*, 1996, **96**, 2205.
22 F. J. Feher, *J. Am. Chem. Soc.*, 1986, **108**, 3850.
23 F. J. Feher, D. A. Newman and J. F. Walzer, *J. Am. Chem. Soc.*, 1989, **111**, 1741.
24 K. Wada, N. Itayama, N. Watanabe, M. Bundo, T. Kondo and T. Mitsudo, *Organometallics*, 2004, **23**, 5824.
25 F. J. Feher and J. F. Walzer, *Inorg. Chem.*, 1991, **30**, 1689.
26 F. J. Feher, T. A. Budzichowski, K. Rahimian and J. W. Ziller, *J. Am. Chem. Soc.*, 1992, **114**, 3859.
27 M. Crocker, R. H. M. Herold and A. G. Orpen, *Chem. Commun.*, 1997, 2411.
28 M. Crocker, R. H. M. Herold, A. G. Orpen and M. T. A. Overgaag, *J. Chem. Soc., Dalton Trans.*, 1999, 3791.
29 M. C. Kung, M. V. Riofski, M. N. Missaghi and H. H. Kung, *Chem. Commun.*, 2014, **50**, 3262.
30 M. Kejik, J. Brus, L. Jeremias, L. Simonikova, Z. Moravec, L. Kobera, A. Styskalik, C. E. Barnes and J. Pinkas, *Inorg. Chem.*, 2024, **63**, 2679–2694.
31 T. Hikino, K. Fujino, N. Sato, H. Wada, K. Kuroda and A. Shimojima, *Chem. Lett.*, 2021, **50**, 1643.
32 R. Duchateau, U. Cremer, R. J. Harmsen, S. I. Mohamud, H. C. L. Abbenhuis, R. A. van Santen, A. Meetsma, S. K.-H. Thiele, M. F. H. van Tol and M. Kranenburg, *Organometallics*, 1999, **18**, 5447.
33 C.-H. Lu, C.-H. Tsai, F.-C. Chang, K.-U. Jeong and S.-W. Kuo, *J. Colloid Interface Sci.*, 2011, **358**, 93.
34 $C_{112}H_{252}O_{52}Si_{32}Ti$, M = 3377.78, monoclinic, space group $P2_1/c$, (#14), a = 20.4538(7), b = 21.7114(6), c = 42.2709(12) Å, α = 90°, β = 90.158(3)°, γ = 90°, V = 18771.6(10) Å^3, T = 93 K, Z = 4, D_{calc} = 1.195 g cm^{-3}, F_{000} = 5328, R_1 = 0.1399, wR_2 = 0.4126, 133642 reflections collected, 33639 unique.
35 J. Přech, *Catal. Rev. Sci. Eng.*, 2018, **60**, 71.
36 N. Kosinov, C. Liu, E. J. M. Hensen and E. A. Pidko, *Chem. Mater.*, 2018, **30**, 3177.
37 M. Crocker, R. H. M. Herold, B. G. Roosenbrand, K. A. Emeis and A. E. Wilson, *Colloids Surf., A*, 1998, **139**, 351.
38 V. A. D. O'Shea, M. Capel-Sanchez, G. Blanco-Brieva, J. M. Campos-Martin and J. L. G. Fierro, *Angew. Chem., Int. Ed.*, 2003, **42**, 5851.
39 S. Marcinko and A. Y. Fadeev, *Langmuir*, 2004, **20**, 2270.
40 K. Momma and F. Izumi, *J. Appl. Crystallogr.*, 2011, **44**, 1272.